Attenuation evaluation, difference between theory and practice

C.C. van Dijk [1,2]
[1] ESC, Energy storage consultancy,
Zoetermeer, the Netherlands

[2] Member of the Dutch Acoustical Society, NAG,
Heerde, the Netherlands
e-mail: **ccvandijk@gmail.com**

Abstract
There is a large difference between the spectral properties of attenuators between different laboratories and between laboratory results and use in practice. There are many standards in order to evaluate a reverberation chamber before the evaluation of an attenuator can be done. The effect of the enclosed volume before the sample and the transition to the sample is much larger and not accounted for in the calculation method / well understood. Under the cut-on frequency the mixture of traveling and standing waves becomes an important factor in the effectiveness of an attenuator, which is not yet used in the analysis. Above the cut-on frequency directivity is an issue. The importance is explained in theory and supported by experimental data. Semi-open attenuators show unrealistically high attenuation properties. This can mathematically be explained from the test method. Even with a high level of uncertainty in the end reflection, the tangential boundary conditions of semi-open attenuators can be derived.

1 Introduction

High differences are measured between the attenuation values of attenuators applied in practice and attenuators in laboratory conditions (see figure 1a-b) [1]. Possible causes are the applicability of different measurement methods, disturbances, flow generated noise and neglected complexities in channels. The Focus in this paper is on the reproducible discrepancies. In other words, can these discrepancies be reproduced by engineering/designing complexities within the channel? This article will also reflect on the validation method for the low frequency evaluations in smaller anechoic reverberation chambers.

2 Physical explanations to divergences in attenuation values

2.1 Acoustic energy model of an attenuator

Before such analytics can be done the energy flows in an acoustic attenuator need to be represented in a more complete simplified model (see figure 2).

Breakout noise can be divided in leakage through the boundary and radiation from a vibrating boundary. The transmitted sound is also a combination of airborne sound and sound transmitted through vibrations.

In acoustic engineering noise is evaluated by subtracting different elements. Elements are often represented by their attenuation value. It is not common to subdivide the attenuation into the attenuation from the conversion of sound power, as occurs in absorption attenuators, and the attenuation from reflection, that

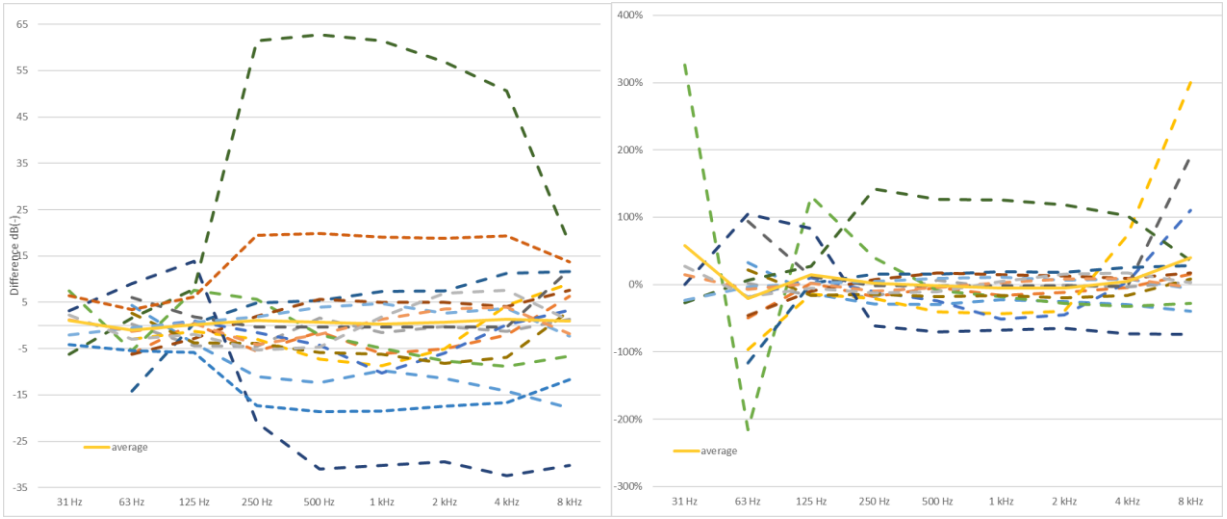

Figure 1a-b: Deviation between lab and in situ attenuation, left in dB, right in % [dB/dB$_{total}$]

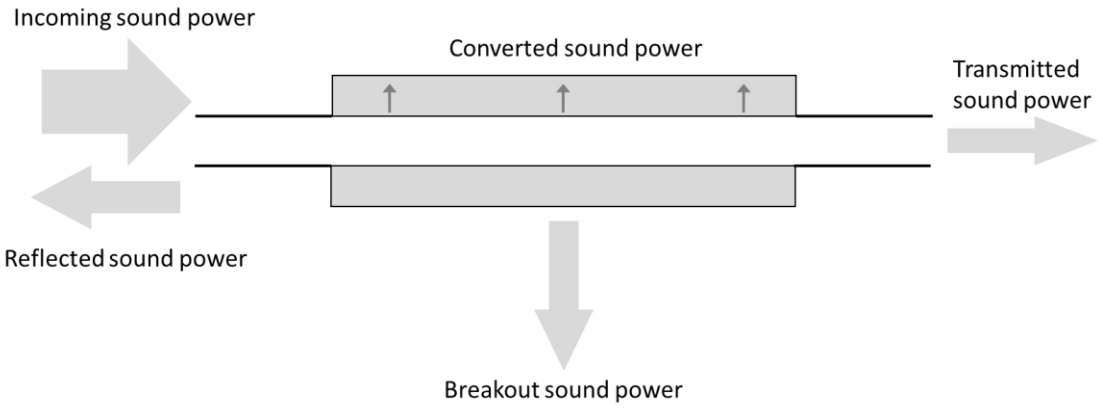

Figure 2: Schematic of different paths the sound power takes around an attenuator

occurs in reflective louvres, bends and, as a result of the difference in wave propagation, at the end reflection. In pure reflective elements, sound power is not converted into different forms of energy.

2.2 Theoretical implications of multiple sequential reflections without absorption

When an attenuation value is pure reflective, The forward partial N of element i equals:

$$N_i = 10^{-(D_i/10)} \tag{1}$$

Where D_i is the attenuation value of reflective element i.

The backward partial equals:

$$1 - N_i \tag{2}$$

When only one reflective attenuator is present and the reflection from the source can be neglected the forward potential is the same as the forward partial, and i =1. The forward potential of the 2nd attenuator (i = 2) is more, because of reflections from the source side. The effect of reflections can be rewritten using a Taylor series:. The forward potential of the 2nd attenuator equals:

$$p_{fi} = N_i + N_i \left(\frac{1}{\frac{1}{(1-N_i)(1-N_{i-1})} - 1} \right) \tag{3}$$

Total effective reflective attenuation of *n* reflective elements in series is a function of the overall transmittance:

$$D_{1-n} = -10\log(T_{1-n}) \tag{4}$$

With the overall transmittance equal to:

$$T_{1-n} = N_1 p_{f2} p_{f3} \dots p_{fn} \tag{5}$$

In appendix A mathematical proof is given that $T_{1\text{-}n}$ equals:

$$T_{1-n} = \frac{N_1 \cdot N_2 \cdot \dots \cdot N_n}{(1-n)(N_1 \cdot N_2 \cdot \dots \cdot N_n) + \sum_{i=1}^{n} \frac{N_1 \cdot N_2 \cdot \dots \cdot N_n}{N_i}} \tag{6}$$

This equation is to be used when a series of reflective different attenuation properties is connected in series without significant damping/attenuation in between the series of elements. Bends, weather cowls/louvres, resonance attenuators are examples of such elements. A special example to use this equation is with a noise reducer hose, see figure 3.

2.3 Implementations to an attenuator with a none reflective boundary service

Figure 3: Noise reducer (acoustically insulated) hose

Attenuators with an acoustically soft shell/boundary, such as a noise reducer hose show high values for the attenuation measured in accordance with ISO 7235 [2]. The breakout and converted sound power under the cut-on frequency and the breakout sound power under the cut-on frequency is the same per unit length. The edges of the attenuator are more or less open to sound to propagate outside the reducer hose. Here the mismatch in wave shape can again prevent the full acoustic energy to escape into a larger volume, as a result a substantial part of the acoustic energy can be reflected into the hard duct towards the source (see figure 4). Because this is so similar to the end-reflection, but doesn't occur at the end, it could be called mid-reflection. The acoustic energy that escapes through the soft boundary can be measured in an echoic room. A check must be done to check if the attenuation value is not limited by short-circuiting noise through the echoic reverberation chamber. If the sound pressure level in the echoic reverberation chamber remains much lower than in the noise reducer hose the mid-reflection can be determined:

$$D_{initial} = D_{smallest\ length} - D_{per\ smallest\ length} \tag{7}$$

At 500 mm and 1000 mm long hoses whit a radius such that the cut-on frequency is above 200 Hz are measured;

$$D_{initial;0-160\ Hz} = D_{500} - (D_{1000} - R_{500}) = 2D_{500;0-160\ Hz} - D_{1000;0-160\ Hz} \tag{8}$$

The mid reflection is an entity that is dependent on the design and material properties of the noise reducer hose, and is best derived from experimental data.

In figure 4 all reflective noise (to the source) is assumed not to return into the elements shown in figure 4. In order to achieve this a special absorptive cone or a relatively large absorbing source room can be used.

By subdividing the reflective properties of the noise absorbing hose from the other properties, when only the transmitted sound power is of interest, figure 4 can be represented by figure 6. Meaning the calculation of the effect of reflection can be done by representation of two reflective elements in series and an absorbing sound converting element. Note that the physics behind the mid reflection are the same for both directions. Also note that in a laboratory setting the breakout noise in figure 4 will be evaluated in a different echoic receiving room than the transmitted sound power.

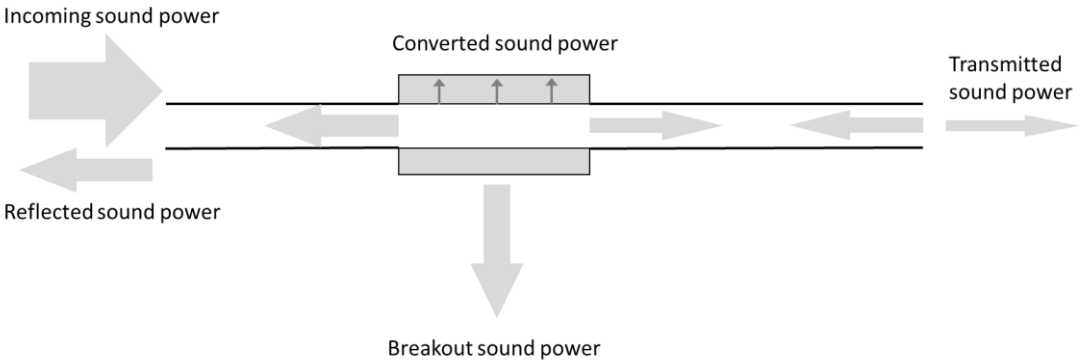

Figure 4: Schematic of different paths around a noise reducer hose

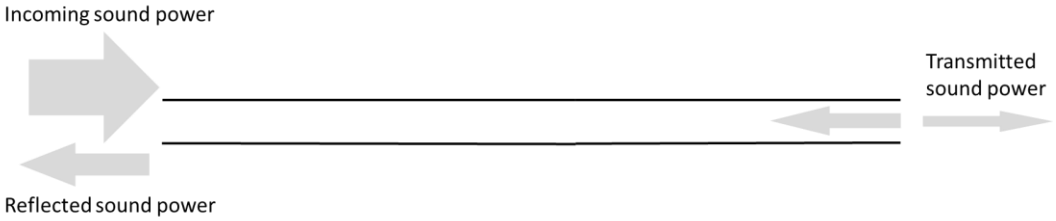

Figure 5: Schematic of reference duct

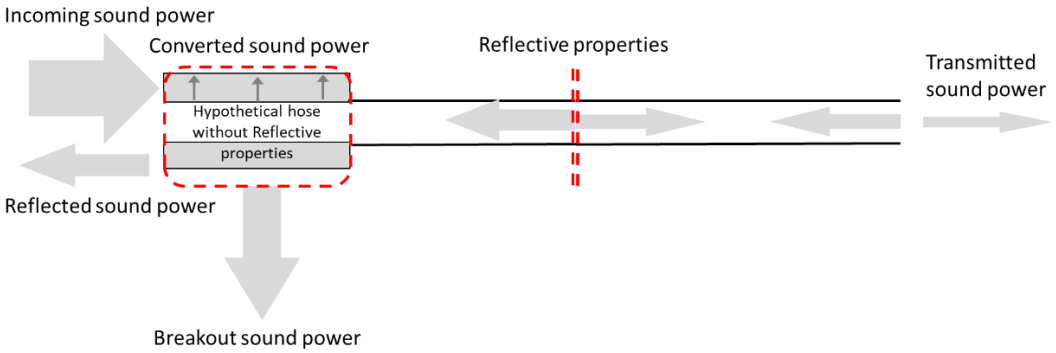

Figure 6: One of two hypothetical alternative representations of figure 4

The end reflection used in this calculative evaluation is given in ISO 7235 [2]:

$$\Delta L_w = 10 \log\left(1 + \frac{\Omega}{\left(\frac{4\pi f S^{0,5}}{c}\right)^2}\right) \tag{9}$$

Where L_w is the sound power level in dB, f is the (mid)frequency in Hz, S is the surface area in m^2, c is the speed of sound in m/s and Ω is the relative area expansion around the end point (4π for all directions, 2π for expansion from the middle of a wall). Note the end reflection increases for an increased value of Ω and a smaller cross sectional area S. However as the size of the cross section area decreases the plane wave purifies, but the smaller size requires less deformation to match a free field. A more detailed evaluation of the end reflection could be an interesting follow up on this study.

Reflections to the source can be assumed fully absorptive.

In fluid dynamics there is a transition region for a flow in a duct to become fully laminar or turbulent. A similar effect may be applicable in ducts before the sound wave is plane, resulting in a different mid-reflection for different sides and the end reflection. The value of Ω can also differ for both sides of the mid reflection, when the noise reducer hose is not placed in the middle of the echoic room. These details are unavailable in the example that is used in this paper. Ideal symmetric conditions are assumed. First the initial Damping can be calculated using eq. 7. The initial damping is caused by an additional reflection that is a surplus on top of the end-reflection. Relating the initial damping to the total reflection by eq. 6 with $n = 2$ minus eq. 9:

$$D_{initial} = \frac{10^{-\frac{D_{end}}{10}} \cdot 10^{-\frac{D_{mid}}{10}}}{10^{-\frac{D_{end}}{10}} + 10^{-\frac{D_{mid}}{10}} - 10^{-\frac{D_{end}}{10}} \cdot 10^{-\frac{D_{mid}}{10}}} - D_{end} \tag{10}$$

With D_{mid} the mid reflection. Rewriting eq. 10 the mid reflection is:

$$10^{-\frac{D_{mid}}{10}} = \frac{10^{-\frac{D_{initial}+D_{end}}{10}} \cdot 10^{-\frac{D_{end}}{10}}}{10^{-\frac{D_{end}}{10}} - 10^{-\frac{D_{initial}+D_{end}}{10}} + 10^{-\frac{D_{initial}+D_{end}}{10}} \cdot 10^{-\frac{D_{end}}{10}}} \tag{11}$$

The data can only be used when there is no significant short-circuiting, and the breakout and converted sound power is similar for each unit of length, which can only be in a pure plane wave. With short-circuiting is meant that noise gets into the echoic chamber and then re-enters the duct. The longer the sample and the higher the straight through attenuation, the higher the chance on leakage. Therefore in Table 1 only the 63 Hz octave-band was considered [3]. Ideally shorter attenuators are compared, however only for nonwoven 200, 250 and 315 mm, the wall reductions (breakout noise) are available.

In table 1, note that a maximum underestimation is mentioned. This means when the attenuator diameter is the same as the end diameter, both the mid-reflection and the non-reflective are available. When there was an end-reflection in the test setup. The mid-reflection replaces the initial insertion loss, which will result in an increase of the effective insertion loss. After table 1 the end-reflection is based on a 315 mm duct end-reflection with Ω equals 2π.

When we take the example of an element with a mid-reflection in a certain frequency of 7 dB, and we test in accordance with ISO 7235 [2], the chosen end-reflection of the duct has an influence. When the end-reflection is 15 dB or 0 dB, the total reflection is respectively 15.5 and 7 dB (eq.5). Subtracting the reference tube with respectively 15 and 7 dB, shows the effect of reflectivity to the insertion loss is 6.5 dB when a low end-reflection is chosen instead of a high end-reflection. This is over 90% of the mid-reflection. If there is a small end-reflection and a high mid-reflection. Note that [2] limits the admissible reflection coefficient (seen from the position of the test object). However the check-up procedure is defined for an element with a 2 m^2 cross-section where there is little influence from the end-reflection.

In table 1 an overestimation is mentioned. The overestimation reflects on the correction for the end-reflection. The sound power in the test-element is assumed to be equal to the sound power after the end-reflection (in the reverberation chamber) plus the end-reflection, while in fact the mid-reflection prevents the end-reflection from entering the test sample in full. In table 1 an overestimation of 21, 23 and 24 dB is mentioned for respectively 200, 250 and 315 mm for 63 Hz. When compared to the breakout noise / wall reductions, the conclusion needs to be drawn that the overestimation as a result of the mid-reflection is overestimated by a minimum of respectively, 0, 1 and 3 dB, see table 2. In other words when we correct for the mid-reflection based upon the initial dampening based upon samples from only 3 and 1 m length the end result has likely suffered from short-circuiting. If any significant noise re-enters from the echoic chamber into the 3 m duct, the insertion loss is limited by leakage and the insertion per unit length is underestimated, resulting in an overestimation of the Initial dampening. Note that when the end reflection is overestimated,

VDI 2081 [5],[8] suggests it is limited to 15 dB, which contradicts ISO 7235 [2], the mid-reflection will also be overestimated, see figure 7.

Table 1: Hypothetical mid reflection from a dataset [3] of 63 Hz

diameter [mm]	D 0,5 m [dB]	D 1,0 m [dB]	D 3,0 m [dB]	$D_{initial}$ [dB]	D_{end} = 6.8 dB			D_{end} = 9.3 dB		
					D_{mid} [dB]	max. over [dB][1]	max. under [dB][2]	D_{mid} [dB]	max. over [dB][1]	max. under [dB][2]
DEC [3] nonwoven 25 mm				Theoretical data from dataset						
200		10.7	17.3	7.4	13.5	20.9	6.1	15.9	23.3	8.5
250		12.9	22.4	8.15	14.4	22.5	6.2	16.8	24.9	8.6
315		16.6	31.7	9.05	15.4	24.4	6.3	17.8	26.9	8.8
DEC [4] AKUDEC 25 mm				Theoretical data from dataset						
80	11.2	13.8		8.6	14.9	23.5	6.3	17.3	25.9	8.7
100	11.9	9.5		14.3	21.0	35.3	6.7	23.4	37.7	9.1
125	6.3	12.4		0.2	0.9	1.1	0.7	1.5	1.7	1.3
130	8.3	11.1		5.5	11.2	16.7	5.7	13.5	19.0	8.0
160	10.2	14.6		5.8	11.6	17.4	5.8	13.9	19.7	8.1
200	9.2	11.1		7.3	13.4	20.7	6.1	15.8	23.1	8.5
250	10.2	14.2		6.2	12.1	18.3	5.9	14.4	20.6	8.2
315	9.2	10.8		7.6	13.7	21.3	6.1	16.1	23.7	8.5

[1] maximum overestimation of the wall reduction as a result of the maximum deviation in reflective properties
[2] maximum underestimation of the insertion loss as e result of the interaction between different reflections

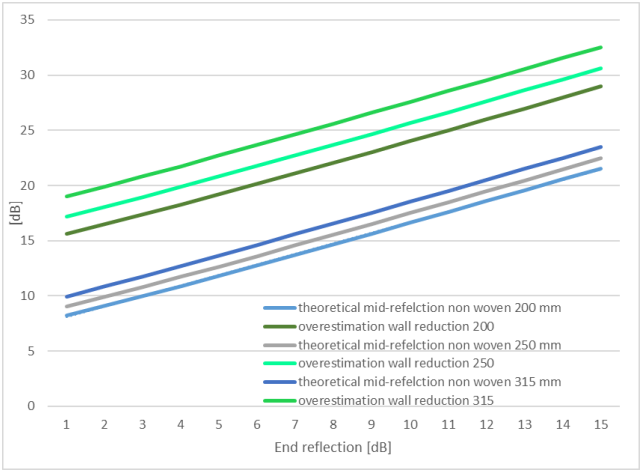

Figure 7: Effect of the real end-reflection on the derived mid-reflection and the deviation in wall reduction

Therefore a thought experiment is proposed. First it is assumed that mid-reflection doesn't exist. Now a conflict arises between the much higher wall reduction in the 63 Hz octave band than in mid-frequencies beneath the cut-on frequency and the fundamental physics. Lower frequencies can more easily bend and can travel through wool with less conversion. Lower frequencies therefore cannot have a higher wall reduction than other frequencies below the cut-on frequency. The reason for this is the correction form the end-reflection. If there is no end-reflection, the wall reduction in 63 Hz decreases 7 or 9 dB, than the wall reduction is still at least 4 till 7 dB more than in 500 and 1000 Hz. The best strategy is to use the measured

wall reduction of 3 dB on a similar material in 63 Hz, and compare this to the wall reduction according to three different hypothesis, see table 2 (where $\Omega = 2\pi$).

Table 2: Comparison of wall reduction between different reflection theories (control value = 3 dB)

	ISO 7235 [3]		
	No reflections	No mid-reflection	Symmetric mid- and end-reflection
200	15	22	1
250	16	23	0
315	13	20	-4

In conclusion the use of a pure symmetric mid- and end reflection is the most accurate. The negative values in table 2 mean a negative wall reduction, which cannot be expected.

- These comparisons should be done with shorter samples;
- The end-reflection in ISO 7235 [2] should be rewritten in an equation that is more widely applicable and takes into account limiting factors.

It is logical to consider when there is so little resistance that the acoustic wave can expand easily and the mismatch in the mid-reflection is similar to the end-reflection, the mid-reflection can exceed the end-reflection when the vibrations of the shell help to increase the mismatch, although in general, when the diameter is the same, lower values for the mid-frequencies should be expected than for the end-reflection.

The effect of the length of the duct between the mid- and the end-reflection could have a significant impact and should be studied in more detail.

One original aim of this study was to quantify the benefits of an open shell attenuator to the transfer of low frequency sound waves. After the reflection model in Chapter 2.2 was accompanied with an exact solution, the infinity of interacting reflections could be accounted for. This led to higher values for the mid frequency. The potential short circuiting because of the length of the sample and potential overestimations on the reflections between mid- and end-reflection resulted in still unrealistic values for the wall reduction. Making a full energy tracing futile.

Note that in ISO 7235 [2] the use is prohibited for reactive silencers. Reactive silencers also incorporate strong reflective properties. A temporary solution could be to extend the exclusion to attenuators with a soft boundary shell, because of their reflective properties.

3 Evaluation of the reverberant receiving room for LF use

A client has its' own small laboratory. The echoic receiving chamber is originally square, one wall is equipped with a diffuser covering 2/3rd of the height of the room, breaking up the square. Another 5 diffusers are located around three top corners and in the middle. The reverberation time shows little variation for 12 different locations. One costumer required the validation of the low frequency attenuation from 25 Hz and upwards. The specific attenuators were 9.3 x 3.2 x 2.1 m and 2 times 2.375 x 3.15 x 2.3 m (W x H x L). These wouldn't fit in any laboratory. Downsizing the attenuators in symmetric parts would result in a different character of the sound field in the test sample in low frequencies, that could have an effect on the insertion loss, see ch.4. The receiving echoic chamber is too small according to ISO 7235 [2], but so are the receiving echoic chambers of bigger laboratories in the Netherlands. ISO 7235 [2] refers to ISO 3741 [6] where the receiving room can be evaluated. Because the size of the echoic reverberation room is 4.9 x 3.7 x 2.5 m = 45.2 m^3, the standard deviation from 25-125 Hz 1/3rd octave band was evaluated. For the evaluation at least 6 source positions need to be evaluated, the source positions need to be placed 1.5 m from the wall and the evaluation position at least 0.8 m from the source. As shown in figure 8 with four out of six microphone positions, this doesn't leave a lot of measurement area for comparison. Hence the omnidirectional source was replaced by a unidirectional source that were positioned as shown in figure 9. The standard deviation for the 1/3rd octave bands is under 100 Hz under 3.9 dB and under 200 Hz under

3 dB and therefore within limits, see table 3. The reverberation chamber is admissible for evaluation from 25 Hz and above. Note that the source position in the actual test has a stronger line with the length of the chamber, which is no beneficial, see figure 10.

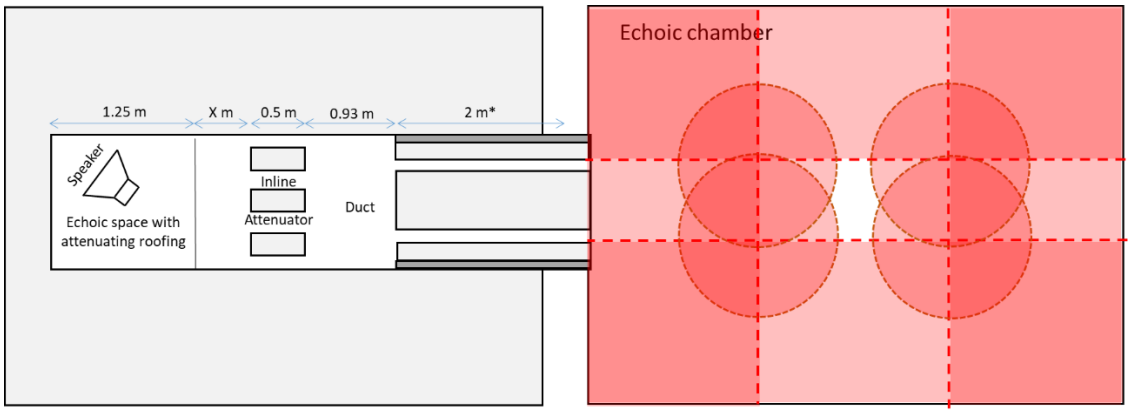

Figure 8: Test setup (left) and limitations to the evaluation of the reverberant room (right)

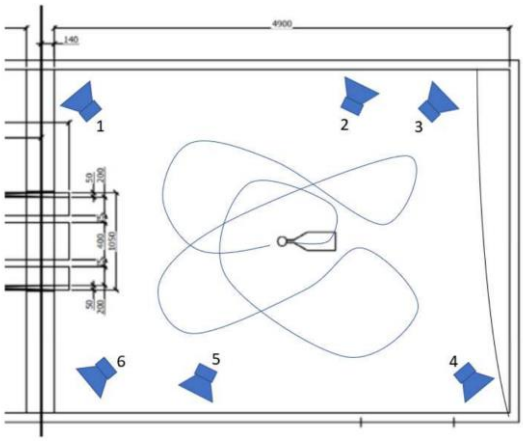

Figure 9: source positions and measurement area for the evaluation of the standard deviation

Table 3: standard deviations for the receiving chamber

25 Hz	1.3	50 Hz	1.6	100 Hz	2.5
31 Hz	2.4	63 Hz	1.9	125 Hz	3.0
40 Hz	1.9	80 Hz	1.6		

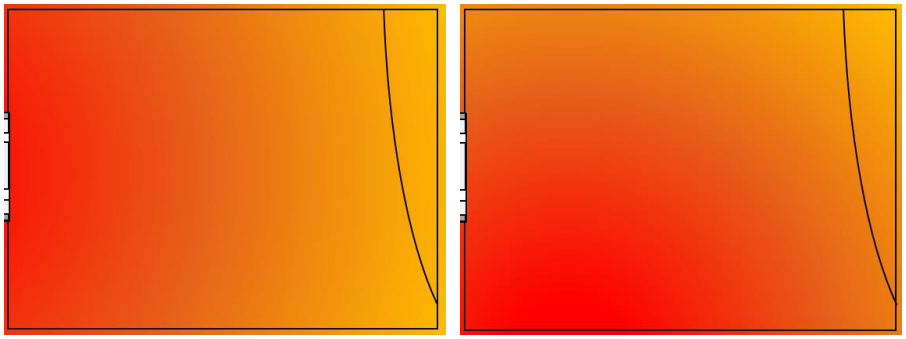

Figure 10: (left) expansion from actual source (right) expansion from pos. 5 (figure 9)

4 Effect of the test sample dimensions and place on insertion loss

In this chapter not the reflection itself, but the effects of the resulting standing wave is discussed. The same case as in ch.3, see figure 4, is used for the analysis of two different splitter attenuators. The insertions loss of one of the attenuators was lower in the 125 Hz than in previous tests, while the insertion loss in the 31 Hz was higher than required. From previous experience [1] a relation between the positioning of the attenuator around a standing wave and the insertion loss was expected. Friction losses only occur when there is transportation to a friction medium, thermos-acoustic effects only take place when there is both transportation and pressure fluctuation. Sound is a combination of velocity and pressure fluctuations. If part of the sound propagates as a standing wave the energy conversion in absorptive attenuators is proportional to the velocity fluctuation squared. The effective attenuation becomes:

$$D_{standing\ wave} = 2D_0 \int_{x_1}^{x_2} sin^2\left(\frac{2\pi x}{\lambda}\right) dx \qquad (12)$$

Where D_0 is the Attenuation under 'normal' circumstances, λ is the wavelength and x_1 and x_2 are the one dimensional position of the attenuator with the hardest boundary as a reference point, see figure 11.

Therefore it was decided to stretch the setup by 0.5 m and limit the height in order to prevent pressure nodes around 125 Hz around the attenuator. The results are given in table 4, where X refers to the length in figure 8.

Table 4: Insertion loss (A & B; X = 0.025 m: A* & B*; X = 0.525 m)

	31 Hz	63 Hz	125 Hz	250 Hz
A 1	11.2	22.5	31.4	38.2
B 1	11.3	25.5	27.6	40.0
A* 2	*8.0*	*23.6*	*30.4*	*36.5*
A* harder boundary 3	*5.2*	*24.9*	*30.7*	*35.2*
B* harder boundary 3	*9.5*	*27.2*	*28.9*	*38.1*

First the noise is split in a standing wave and a plane wave. The plane wave is the initial sound wave. The standing wave originates from the noise that is reflected between the source area and the exit of the attenuator in the reverberation chamber, when it has been exposed to the boundary conditions. Both boundaries are open, but the opening to the reverberation chamber is much larger, therefore the maximum pressure amplitude is situated at the far end of the source area, see figure 4. Note that the modes as well as the pressure conditions throughout the sample can vary, except for the hardest boundary on the left.

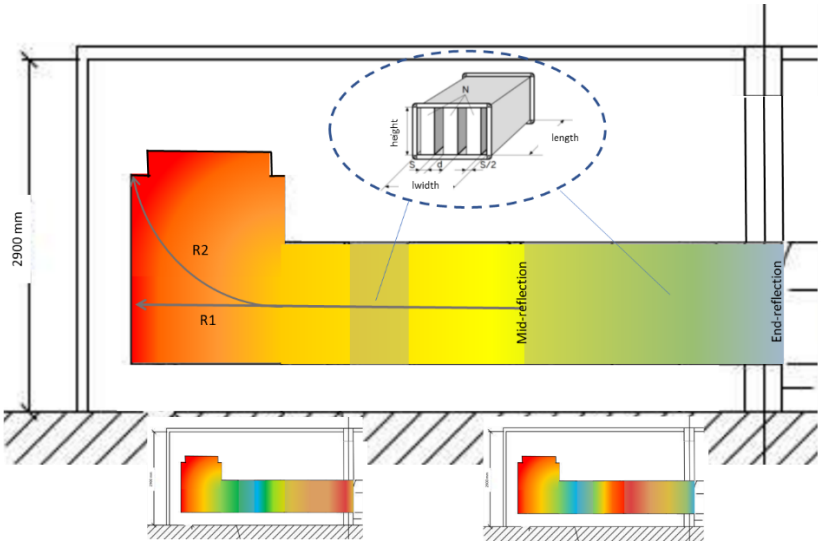

Figure 11. Maximum pressure points in red with two distances R1 & R2

For the end-reflection eq. 9 was used with S the height of the opening times the difference between the far left end the far right of the opening. The reflection on the boundary on the left as well as the reflection on the face surface of the attenuator within the channel is derived from the equation of the cross sectional change as mentioned in VDI 2081 [5],[8]:

$$\Delta L_w = \frac{10\log\left(\frac{S_1}{S_2}+1\right)^2}{\frac{4S_1}{S_2}} = D_{reflection} \tag{13}$$

Just like in chapter 2, the reflections, both end-reflection and wall reflection could be quantified. Now the standing wave relative to the plane wave can be expressed as:

$$SW = \left(\frac{1}{\frac{10^{-\frac{D_{standing\ wave}}{10}}}{10^{-\frac{D_{reflection1}}{10}} \cdot 10^{-\frac{D_{reflection2}}{10}}} - 1} \right) \tag{14}$$

Note that because of the two different values/locations for reflection 2 and the two different values R1 and R2 (figure 4), there are four scenarios for SW. The highest values are presented in figure 12. The average attenuation in figure 13 from eq. 12-16 was weighted in accordance with the SW value (eq. 14) and is presented together with the results from the maximum value for SW.

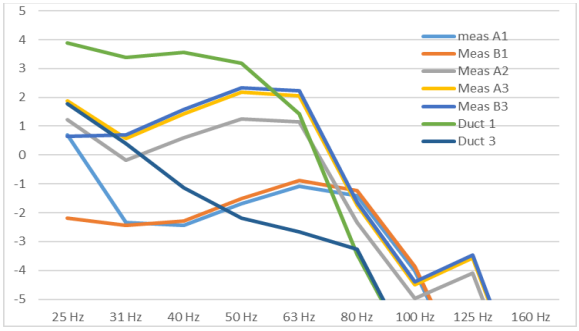

Figure 12. Maximum standing wave in dB

The effective attenuation of the sample, but also of the modal filter (attenuator) in both the reference channel and in the setup with the test sample equals:

$$D_{sample/mf} = -10\log\left(\frac{10^{-\frac{D_0}{10}} + SW \cdot 10^{-\frac{D_{standingwave}}{10}}}{1+SW}\right) \tag{15}$$

Note that the modal filter (mf) is also in the possession of D_0 properties.

The measured attenuation [2] then becomes:

$$D = D_{smaple} + D_{mfsample} - D_{mfduct} + D_{endsample} - D_{endduct} \tag{16}$$

Eq. 12 till 16 are evaluated for each 1/3rd frequency band, for all two attenuators in all three setups, see figure 13. In figure 13 the shortcomings from 25 to 40 Hz of attenuator A are well predicted while no significant shortcomings in these frequencies were predicted for attenuator B. Even B* 3 that shows the lowest attenuation in 25-40 Hz was predicted to attenuate 1 dB worse than A 1. However the difference in reality was more than 1 dB. Higher frequency results are also shown in figure 13. Note that R1 and R2 in figure 4 in reality produce a range of potential reflections, instead of two and that the speed of sound is higher in attenuators and in the shell. Higher frequencies are very perceptive to this small influences on the dimensions because of their relation to the wavelength. More interestingly, because of the high nominal attenuation very small proportions of standing waves compared to the plane wave can have a strong influence. This influence potential increases as the attenuation length decreases.

In another project in practice a strong standing wave dramatically improved the octave band attenuation value in 31-125 Hz with 10-20 dB. Note that the pattern is repetitive and a minimum length is no prevention.

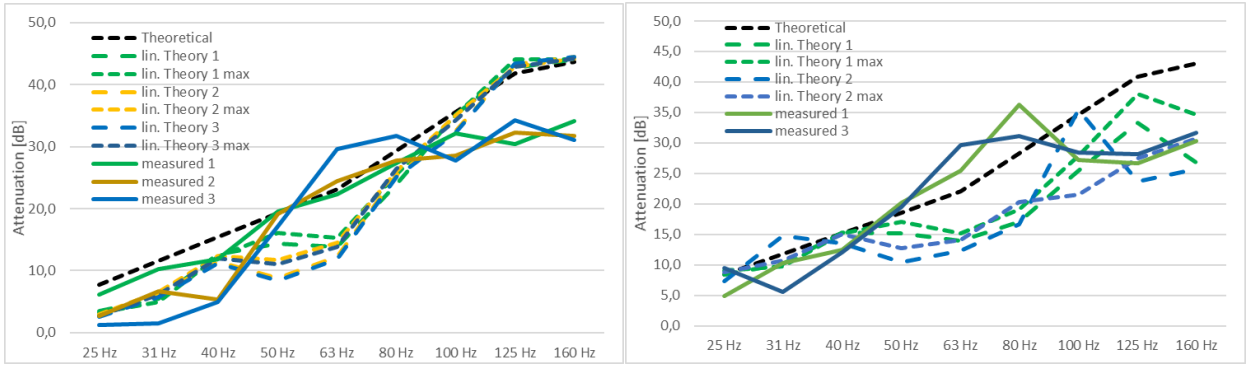

Figure 13. (left) Attenuator A (right) Attenuator B, 1/3rd octave band calculated and measured values

5 Effect of directivity on high frequency insertion loss

In line with the shielding effect derived from Fresnel [7], the potential lack of shielding was taken into account in attenuators [4]. This effect was called leakage and is directly related to the direction of the sound field. From field studies the effect of leakage was found to be easily between 10 and 32 dB, Because leakage was introduced as a predictive tool, the field results were used to generate a best fit between theory and practice by adjusting the constant of Fresnel from 0.059 to 0.047 [4]. More measurements were taken where a small leakage effect was expected. In all field data the directive sound is mixed with reverberant sound. First the Fresnel constant was re-established in all equations of the previous work [4], resulting in a probability function of the mid frequency f_m and necessary radius r, for scenario I [4]:

$$\eta(r) = \frac{(2-r_1^2)+\left((2-r_1^2)^2-4\right)^{0,5}+(2-r_2^2)+\left((2-r_2^2)^2-4\right)^{0,5}}{\frac{4}{fm*0.059}} \tag{17}$$

for scenario II and III [4]:

$$2\eta(r) = \frac{(2-r_1^2)+\left((2-r_1^2)^2-4\right)^{0,5}-(2-r_3^2)-\left((2-r_3^2)^2-4\right)^{0,5}}{\frac{2}{fm*0.059}} \tag{18}$$

Not giving any details about the different mechanisms in which the attenuators can be completely avoided and leakage is present. Leakage can only come from a directional sound field, assuming the reverberant sound field to be omnidirectional. Leakage can only take place in the splice with thickness b and not on the splitter head with thickness a.

As a result of the use of 0.059 instead of 0.047, the calculated leakage was significantly more than the measured leakage. However all reference projects have a source in a reverberant field. In this field either the reverberant sound or the reflective sound from the splitter hard face can interact with the directive soundwave front. After calculating with different correction factors, the correction factor that considers both the influence of interaction with the reverberant field and the reflective attenuator face surface ratio has shown the best fit. This is logical, because a reverberant sound field interacts with the direct sound field. The overall leakage *G'* was a function of the integrated leakage over the angles corrected for the ratio between splice area over total face area and in room acoustics for the fraction of direct sound power over all sound power:

$$G' = G_0\left(\frac{b}{b+a}\cdot\frac{10^{\left(\frac{Li_{direct}}{10}\right)}}{10^{\left(\frac{Li_{direct}}{10}\right)}+10^{\left(\frac{Li_{reverberant}}{10}\right)}}\right)^2 \tag{19}$$

Where L_w is the sound power acting on the attenuator, being either direct or reverberant sound. By using eq. 18 diffraction on the silencers edge is neglected, because leakage has more influence on the higher frequencies with less influence of diffraction. With G_0 the sum of all probabilities of leakage.

Now the attenuation with leakage *D''* as a function of the attenuation without leakage *D* becomes:

$$D' = -10\log\left(10^{-\left(\frac{D}{10}\right)} + 10^{-\left(\frac{-10\log(G')}{10}\right)}\right) \quad (20)$$

In a simulation tool a more accurate interaction may already be present, the aim of this paper is to establish an acceptable level of accuracy for lumped parameter analysis. The calculated spectral attenuation with and without leakage can predict a 8, 14 or even 30 dB deficiency in attenuation values, see figure 14. Note that in most projects there is no significant influence of leakage, in reality (as shown in figure 1) as well as in the calculation.

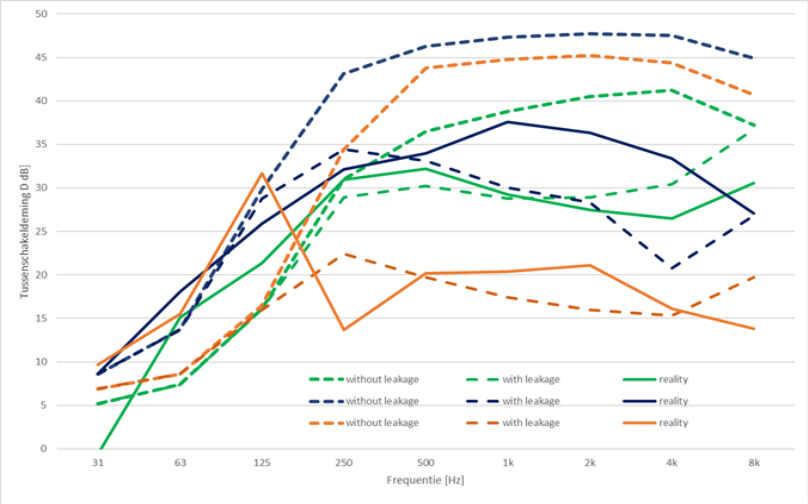

Figure 14: Comparison of three projects with a calculation with and without leakage

Note that eq. 20 needs to be solved for each specific sound source in a reverberant room.

During work in an internal area behind an attenuator an ambulance approached. As the ambulance came closer the noise from the silencer became more silent. In figure 15 this situation was recalculated using the equations for leakage. The frequency was assumed 2000 Hz, the attenuation value 55 dB and the splice distance 150 mm and the splitter thickness 250 mm. The attenuator is 3 m wide and the ambulance approaches 0.5 m from the edge, in line with the attenuator splice length until 1 m distance.

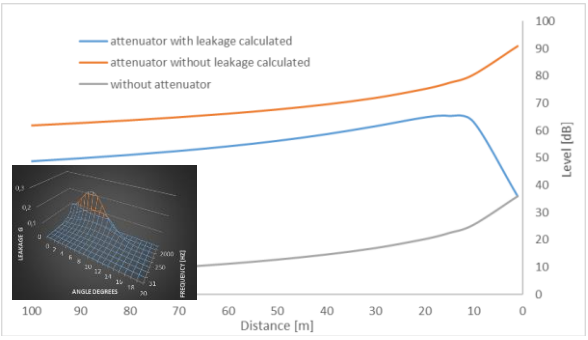

Figure 15: Comparison of three projects with calculations with and without leakage

When this knowledge is reflected upon the measurement procedure, section 5.4.2.3 [2] provides minimum expansion lengths for the transition element connecting either the sample to the channel or the channel to the source. This provides well developed sound fields for testing. In reality this section is often overlooked and is therefore not respected. When the channel is long and narrow and the attenuator is substantial in size leakage could easily reduce the attenuation value from 2 kHz onwards with 20 dB. The specific example has been left out, because the numbers are not more substantial than in figure 10 and 11. One could suggest to create optimal test conditions (under a strong angle) and add the effect of leakage for specific applications, resulting in a better match between calculations and practice/reality.

6 Summery and conclusions

In laboratory conditions a number of deviations can be intentionally designed that can recreate the large order of magnitude for deviations in practice. All accept one fall within the limitations of ISO 7235 [2].

In order to quantify the airborne sound aspects the problem of infinite reflections of elements with different properties was solved, see eq. 6.

Not accounting for the mid-reflection in soft boundary attenuators can result in a significant underestimation of their attenuation and an overestimation of the wall transmission losses in low frequencies

Standing waves in the sample far beneath the limit can result in serious underestimations of the attenuation properties >10 dB for all frequencies. Strong limitations for the absorbing properties are necessary, ideally the absorption equals 1.0, in practice a minimum of 0.85 for all frequencies seems more feasible.

The minimum length of the channel of 0.5 λ cannot prevent strong effects from standing waves.

The leakage can result in 30 dB less or 60 dB more attenuation. It is well limited by ISO 7235 [2], but the rules are impractical and are sometimes neglected. Ideally leakage is further reduces by the introduction of an additional bend. Than leakage can be re-introduced by calculations based upon the conditions and geometries in which the attenuator is to be placed.

Acknowledgements

This research was made possible by data off assignments from Alara-Lukagro that was given in consent accompanied by publically available data from DEC International. André Hameete and Cees Dingenouts in particular have shared the vision to share this important knowledge. Other people that have either shared the enthusiasm or suffered the absence of the author are also very much appreciated.

References

[1] C.C. van Dijk, “Acoustic validation of calculation software for ducts, panels and acoustic rooms,” in *Proceedings in the 23rd Int. Congress on Acoustics 2019*

[2] ISO 7235: *2009*

[3] DEC International technical documentation 107849 *www.ventvan.ru r2020 10-5-2022*

[4] C.C.van Dijk, and G. Busch, “The use of Fresnel theory to predict attenuator values of attenuators in room acoustics,” in *Proceedings 46th congress edition DAGA 2020*

[5] VDI 2081: Part 1: *July 2001*

[6] ISO 3741: *2010*

[7] J.W. Strutt, and M.A. Baron Rayleigh, *Theory of sound. Macmillan and co.*, London, *1877*

[8] H. Kopp, Schalldämmung von lufttechnischen Leitungen. *VDMA FLT, Frankfurt, Forschungsberichte Heft 16 (1986), S. 51/78*

Appendix

A Mathematical proof and follow up ch.2.2

2nd attenuator inverse forward (i = 2)

$$p_{fi,inv} = N_{i-1} + N_{i-1}\left(\frac{1}{\frac{1}{(1-N_i)(1-N_{i-1})}-1}\right) \tag{21}$$

3rd attenuator forward potential (i = 3) and further

$$p_{fi} = N_i + N_i\left(\frac{1}{\frac{1}{(1-N_i)\left((1-N_{i-1})+(N_{i-1})p_{fi-1,inv}\right)}-1}\right) \tag{22}$$

3rd attenuator inverse forward (i = 3) and further

$$p_{fi,inv} = N_{i-1} * p_{fi-1,inv} + N_{i-1} * p_{fi-1,inv} * \left(\frac{1}{\frac{1}{\left((1-N_{i-1})+N_{i-1}*\left(1-p_{fi-1,inv}\right)\right)*(1-N_i)}-1}\right) \tag{23}$$

Then the overall transmittance of two different pure reflective elements is:

$$T_{1-2} = N_{i-1}\left(N_i + N_i\left(\frac{1}{\frac{1}{(1-N_i)(1-N_{i-1})}-1}\right)\right) \tag{24}$$

$$T_{1-2} = N_i N_{i-1}\left(1 + \left(\frac{(1-N_i)(1-N_{i-1})}{1-(1-N_i)(1-N_{i-1})}\right)\right) \tag{25}$$

$$T_{1-2} = N_i N_{i-1}\left(\frac{N_{i-1}+N_i-N_iN_{i-1}}{N_{i-1}+N_i-N_iN_{i-1}} + \frac{1-N_{i-1}-N_i+N_iN_{i-1}}{N_{i-1}+N_i-N_iN_{i-1}}\right) \tag{26}$$

$$T_{1-2} = \frac{N_iN_{i-1}}{N_{i-1}+N_i-N_iN_{i-1}} \tag{27}$$

When three different pure reflective elements are in series, the total transmittance $T_{1\text{-}3}$:

$$\boldsymbol{N_{i-2}\left(N_{i-1} + N_{i-1}\left(\frac{1}{\frac{1}{(1-N_{i-1})(1-N_{i-2})}-1}\right)\right)\left(N_i + N_i\left(\frac{1}{\frac{1}{(1-N_i)\left((1-N_{i-1})+N_{i-1}\left(1-\left(N_{i-2}+N_{i-2}\left(\frac{1}{\frac{1}{(1-N_{i-1})(1-N_{i-2})}-1}\right)\right)\right)\right)}-1}\right)\right)} \tag{28}$$

Note: $N_{i-2}\left(N_{i-1} + N_{i-1}\left(\frac{1}{\frac{1}{(1-N_{i-1})(1-N_{i-2})}-1}\right)\right) = \frac{N_{i-1}N_{i-2}}{N_{i-2}+N_{i-1}-N_{i-1}N_{i-2}}$

and $N_{i-1} + N_{i-1}\left(\frac{1}{\frac{1}{(1-N_{i-1})(1-N_{i-2})}-1}\right) = \frac{N_{i-2}}{N_{i-2}+N_{i-1}-N_{i-1}N_{i-2}}$

and $\left(N_i + N_i\left(\frac{1}{\frac{1}{(1-N_i)\left((1-N_{i-1})+N_{i-1}\left(1-\left(N_{i-2}+N_{i-2}\left(\frac{1}{\frac{1}{(1-N_{i-1})(1-N_{i-2})}-1}\right)\right)\right)\right)}-1}\right)\right) = \frac{-N_i}{1-(1-N_i)\left((1-N_{i-1})+N_{i-1}-\frac{N_{i-1}N_{i-2}}{(N_{i-2}+N_{i-1}-N_{i-1}N_{i-2})}\right)} = \frac{N_i}{N_i+\frac{N_{i-1}N_{i-2}}{N_{i-2}+N_{i-1}-N_{i-2}N_{i-1}}-\frac{N_iN_{i-1}N_{i-2}}{N_{i-2}+N_{i-1}-N_{i-2}N_{i-1}}}$

$$T_{1-3} = \frac{N_i N_{i-1} N_{i-2}}{(N_{i-2}+N_{i-1}-N_{i-1}N_{i-2})\left(N_i+\frac{N_{i-1}N_{i-2}}{N_{i-2}+N_{i-1}-N_{i-2}N_{i-1}}-\frac{N_i N_{i-1} N_{i-2}}{N_{i-2}+N_{i-1}-N_{i-2}N_{i-1}}\right)} \tag{29}$$

$$T_{1-3} = \frac{N_i N_{i-1} N_{i-2}}{N_i N_{i-1}+N_i N_{i-2}+N_{i-1}N_{i-2}-2N_i N_{i-1} N_{i-2}} \tag{30}$$

Note that N_i, N_{i-1}, and N_{i-2} can change positions without changing the overall outcome, however the local outcome is influenced by the sequence.

Note that for four reflective elements:

$$T_{1-4} = \frac{N_i N_{i-1} N_{i-2} N_{i-3}}{N_i N_{i-1} N_{i-2}+N_i N_{i-2} N_{i-3}+N_{i-1} N_{i-2} N_{i-3}+N_i N_{i-2} N_{i-3}-3N_i N_{i-1} N_{i-2} N_{i-3}}$$

$$= N_{i-2}\left(\boldsymbol{N_{i-1}+N_{i-1}}\left(\frac{\mathbf{1}}{\frac{\mathbf{1}}{(\mathbf{1}-\boldsymbol{N_{i-1}})(\mathbf{1}-\boldsymbol{N_{i-2}})}-\mathbf{1}}\right)\right)\left(\boldsymbol{N_i+N_i}\left(\frac{\frac{1}{1}}{(1-\boldsymbol{N_i})\left((1-\boldsymbol{N_{i-1}})+\boldsymbol{N_{i-1}}\left(1-\left(\boldsymbol{N_{i-2}+N_{i-2}}\left(\frac{\frac{1}{1}}{(1-\boldsymbol{N_{i-1}})(1-\boldsymbol{N_{i-2}})}-1\right)\right)\right)\right)}-1\right)\right)\right.$$

$$\left.\left(N_i+N_i\left(\frac{\frac{1}{1}}{\left((1-N_{i-1})+N_{i-1}\left(\left(\left(1-\left(N_{i-2}\left(N_{i-3}+N_{i-3}\left(\frac{\frac{1}{1}}{(1-N_{i-2})(1-N_{i-3})}-1\right)\right)\right)+N_{i-2}\left(N_{i-3}+N_{i-3}\left(\frac{\frac{1}{1}}{(1-N_{i-2})(1-N_{i-3})}-1\right)\right)\right)\left(\frac{\frac{1}{1}}{\left((1-N_{i-2})+N_{i-2}\left(1-\left(N_{i-3}+N_{i-3}\left(\frac{\frac{1}{1}}{(1-N_{i-2})(1-N_{i-3})}-1\right)\right)\right)\right)(1-N_{i-1})}-1\right)\right)\right)(1-N_i)\right)}-1\right)\right)\right) \tag{31}$$

Concluding T_{1-2}, T_{1-3} and T_{1-4}:

$$T_{1-n} = \frac{N_1 \cdot N_2 \cdot \ldots \cdot N_n}{(1-n)(N_1 \cdot N_2 \cdot \ldots \cdot N_n)+\sum_{i=1}^{n}\frac{N_1 \cdot N_2 \cdot \ldots \cdot N_n}{N_i}} \tag{32}$$